A Macrophage Infection Model to Predict Drug Efficacy Against *Mycobacterium Tuberculosis*

Kaitlyn Schaaf,[1] Virginia Hayley,[1] Alexander Speer,[2,3] Frank Wolschendorf,[1] Michael Niederweis,[2] Olaf Kutsch,[1] and Jim Sun[2]

[1]*Department of Medicine, University of Alabama at Birmingham, Birmingham, Alabama.*
[2]*Department of Microbiology, University of Alabama at Birmingham, Birmingham, Alabama.*
[3]*Department of Medical Microbiology and Infection Control, VU University Medical Center, Amsterdam, Netherlands.*

ABSTRACT

In the last 40 years, only a single new antituberculosis drug was FDA approved. New tools that improve the drug development process will be essential to accelerate the development of next-generation antituberculosis drugs. The drug development process seems to be hampered by the inefficient transition of initially promising hits to candidate compounds that are effective in vivo. *In this study, we introduce an inexpensive, rapid, and BSL-2 compatible infection model using macrophage-passaged* Mycobacterium tuberculosis (Mtb) *that forms densely packed* Mtb/*macrophage aggregate structures suitable for drug efficacy testing. Susceptibility to antituberculosis drugs determined with this* Mtb/*macrophage aggregate model differed from commonly used* in vitro *broth-grown single-cell* Mtb *cultures. Importantly, altered drug susceptibility correlated well with the reported ability of the respective drugs to generate high tissue and cerebrospinal fluid concentrations relative to their serum concentrations, which seems to be the best predictors of* in vivo *efficacy. Production of these* Mtb/*macrophage aggregates could be easily scaled up to support throughput efforts. Overall, its simplicity and scalability should make this* Mtb/*macrophage aggregate model a valuable addition to the currently available* Mtb *drug discovery tools.*

INTRODUCTION

With one-third of the world population latently infected with *Mycobacterium tuberculosis* (*Mtb*), tuberculosis (TB) remains a global health threat. While drug intervention can be successful for the treatment of TB, success is often hampered by long treatment periods lasting over 6 months[1] and the requirement to treat with multiple drugs, a scenario that often leads to lack of compliance.

To be effective, drugs must be transported from the blood compartment to nonvascularized pulmonary lesions and diffuse into necrotic foci through multiple cell types.[2] At the site of infection, *Mtb* remains hidden inside macrophages and/or encapsulated within granuloma structures, a hallmark feature of *Mtb* infection.[3] Finally, drugs have to cross the highly impermeable, lipid-rich cell envelope of *Mtb*,[4] and need to reach their molecular target at adequate concentrations. To further complicate matters, *Mtb* infection often persists long term in a hyperdrug-resistant, latent state.[5] This poses a problem to standard anti-TB drugs since the vast majority of these only target metabolically active *Mtb*. Thus, both tissue penetration capacity and efficacy against latent *Mtb* are two critical parameters that define TB drug potency. A major problem with the successful transfer from discovery to application for *Mtb* drugs is that these parameters have not been given sufficient consideration during *in vitro Mtb* drug screening or the early lead development process.[6,7] The majority of drug screens were performed using extracellular *in vitro* broth-grown single-cell culture assays, in which *Mtb* is actively growing and only the *Mtb* cell membrane acts as a potential diffusion barrier.

More recently, this problem has been recognized and drug screening assays against nonreplicating, latent *Mtb*[8,9] or intracellular *Mtb* have been established,[10–12] but even these more advanced assays do not consider the penetration barriers that drugs encounter in the nonvascularized pulmonary lesions, or the necrotic foci at the site of infection. The ability to examine direct tissue penetration of drugs is only achieved using advanced experimental approaches and high-end instrumentation such as matrix-assisted laser desorption/ionization mass spectrometry imaging.[13–15] These highly advanced methods have been used to generate drug penetration profiles in *in vivo* lung lesions and granulomas,[13] but are limited to a few laboratories in the world due to specific instrumentation requirements, and as such are prohibitively expensive to be applied during the early drug development process.

Even a low-throughput drug susceptibility assay that could simultaneously indicate the efficacy of candidate compounds to diffuse through physiologically relevant penetration barriers and exert activity against latent *Mtb* would significantly add to the currently available research tools to prioritize discovered hit compounds.

MATERIALS AND METHODS

Cell Culture and Reagents

THP-1 monocytes (ATCC TIB-202) were maintained in the RPMI 1640 medium supplemented with 2 mM L-glutamine and 10% heat-inactivated fetal bovine serum (FBS) at 37°C in a humidified atmosphere of 5% CO_2. FBS was obtained from Life Technologies. Resazurin, rifampicin, streptomycin, moxifloxacin, ciprofloxacin, gentamicin, clarithromycin, and cycloserine were purchased from Sigma-Aldrich. Hygromycin B was purchased from Calbiochem.

Bacteria and Plasmids

The *M. tuberculosis* H37Rv-derived auxotroph strain $mc^2$6206 was grown in the Middlebrook 7H9 medium (Difco) supplemented with 0.2% glycerol, 0.02% tyloxapol, and 10% OADC (Remel) or on Middlebrook 7H10 plates supplemented with 0.5% glycerol and 10% OADC. Growth media of the auxotrophic *M. tuberculosis* strain were supplemented with 24 μg/mL pantothenate and 50 μg/mL L-leucine.[16] The plasmid pMN437[17] was transformed into *M. tuberculosis* $mc^2$6206 to express GFP, which was used for all experiments in this study. Nonreplicating nutrient-starved *Mtb* was cultured by replacing the normal *Mtb* media of a culture at $OD_{600} = 1.0$ with phosphate-buffered saline, 0.02% tyloxapol, 24 μg/mL pantothenate, and 50 μg/mL L-leucine. Cultures were left standing at 37°C for 4 weeks before drug susceptibility testing. Single-cell *Mtb* for drug susceptibility testing was obtained by water bath sonication (Fisher FS-60; 130 W; 3 × 10 s pulses) of broth-grown *Mtb* cultures.

Infection Protocol

M. tuberculosis $mc^2$6206 growing in log-phase was quantified by optical density measurement at 600 nm using the conversion of 3×10^8 bacteria per mL for OD 1.0. The amount of bacteria required to achieve a multiplicity of infection (MOI) of 25 were washed, resuspended in cell culture media, and added to the THP-1 cultures. Monocytes and *Mtb* were then resuspended together to ensure even exposure of the monocytes to *Mtb*. Media were changed every 2–3 days during an infection time of 10–14 days.

Resazurin Microtiter Assay

Mtb-infected THP-1 aggregates from 10- to 14-day old cultures were harvested and resuspended in *Mtb* growth media. As the strain of *Mtb* used in this model neither replicates nor is killed during this infection period, we adjusted the bacteria concentration to 6 million/mL based on initial *Mtb* input on the day of infection and the total culture volume during harvest. At the same time, *in vitro* broth-grown single-cell *Mtb* cultures were adjusted to a final bacteria concentration of 6 million/mL corresponding to an optical density at 600 nm of 0.02 (using the conversion of 3×10^8 bacteria per ml for OD 1.0). *Mtb* derived from *Mtb*/macrophage aggregates (*Mtb*-aggregate) and *in vitro* broth-grown single-cell cultures (*Mtb*-single) were distributed to 96-well plates in a final volume of 200 μL containing antibiotics in a range of concentrations. The 96-well plates were incubated for 5 days at 37°C. Then, 20 μL of resazurin dye mixture was added to achieve a final concentration of 100 μM resazurin and 0.5% Tween 80 and incubation at 37°C was continued for another 16–30 h before the plates were analyzed by a Synergy HT plate reader (BioTek). Conversion of the indicator dye resazurin into resorufin with a fluorescence emission peak at 590 nm served as a marker for bacterial growth. Refer to *Table 1* for detailed protocol.

Nile Red Staining

M. tuberculosis bacilli were extracted from *Mtb*/macrophage aggregates by water bath sonication for 5 min. Then, *Mtb* was smeared onto glass slides and heat fixed. Nile Red (Acros Organics) was dissolved in ethanol and used at a working concentration of 10 μg/mL to cover the fixed *Mtb* on slides for 15 min at room temperature. Slides were gently washed with water and mounted with a coverslip in FluorSave mounting solution (Millipore).

Table 1. Resazurin Assay Protocol

Step	Parameter	Value	Description
1	Titrate drugs	100 μL	Twofold serial dilutions in appropriate concentration range
2	Plate *Mtb*	100 μL	Broth-grown or *Mtb*/macrophage aggregates (6 million/mL)
3	Incubation time	5 days	37°C without shaking
4	Resazurin addition	20 μL	Final concentration: 100 μM resazurin and 0.5% Tween 80
5	Assay development	16–30 h	37°C without shaking
6	Assay readout	530/590 nm	Measure fluorescence on plate reader

© MARY ANN LIEBERT, INC.

Fluorescence Microscopy

For Nile Red staining, imaging was performed using an Axiovert 200 microscope (Carl Zeiss) equipped with a 100×/1.4 Plan-Apochromat (Carl Zeiss) and the filter set 49004-ET-CY3/TRITC (Chroma). Images were recorded using an AxioCam MRc camera (Zeiss) coupled to Axiovision v4.5 software (Carl Zeiss). For automated imaging of *Mtb*/macrophage aggregation within 96-well plates, the Cytation 3 Cell Imaging Multi-Mode Reader (BioTek) fitted with 2.5× or 20× objectives and the GFP filter set were used. To examine *Mtb*/macrophage aggregates, PE-conjugated antibody to ICAM-1 (BD Biosciences) and the cell viability staining dye 7-amino-actinomycin D (7AAD; eBioscience) were used at a dilution of 1:20 according to manufacturer's protocol. Thereafter, cells were imaged with the EVOS FL Cell Imaging System (Life Technologies) with the combination of GFP/RFP light cubes at 20× magnification.

Table 2. MIC90 of Anti-TB Drugs Against *Mtb* H37rv Compared to *Mtb* mc^{2}6206

	MIC (μg/mL)	
Drugs	*Mtb* H37Rv	*Mtb* mc^{2}6206
Rifampicin	0.05	0.1
Isoniazid	0.04	0.04
Ethambutol	2	2
Kanamycin	5	2.5
Moxifloxacin	0.25	0.25
Cycloserine	6	6
Tetracycline	12	6
Ampicillin	160	160

RESULTS AND DISCUSSION

To provide an efficient experimental tool for improved *in vitro Mtb* drug development, we established a simple *Mtb* infection model that is amenable for early hit verification or even drug screening. For reasons of cost efficiency and general usability, it is highly desirable to use a mycobacteria strain that is suitable for work under BSL-2 conditions, but this strain needs to remain as closely related to the model strain, *Mtb* H37Rv, as possible. While the commonly used *Mtb* surrogates *M. bovis* BCG and *M. smegmatis* satisfy the BSL-2 condition, these strains are not closely related to *Mtb*. BCG is an attenuated vaccine strain derived from *M. bovis* that does not naturally infect humans, while *M. smegmatis* is a rapid-growing mycobacterium that lacks most *Mtb* virulence genes and has different antibiotic resistance profiles compared to *Mtb*. Thus, we chose to use *Mtb* mc^{2}6206 (Δ*panCD*, Δ*leuCD*), a specific derivative of H37Rv[16] that retains all but four genes, *panCD* and *leuCD*, which are neither implemented in virulence nor drug resistance. The auxotrophic *Mtb* mc^{2}6206 strain is a BSL-2 organism that can be handled in almost any laboratory. Its utilization massively reduces experimental time investment and costs compared to studies utilizing *Mtb* H37Rv, which requires handling in BSL-3 facilities. *Mtb* mc^{2}6206 maintains the RD-1 locus (absent from BCG), which plays a major role in *Mtb* virulence and granuloma formation.[18] Importantly, we determined the minimal inhibitory concentrations (MIC) of standard TB drugs on *Mtb* mc^{2}6206 and show that the strain's requirement for supplementation with L-leucine and pantothenate to replicate does not affect its drug susceptibility profile compared to the parent H37Rv strain (*Table 2*). Furthermore, auxotrophic *Mtb* strains have already been used in well-established drug evaluation studies for *Mtb*.[19–21] For our experiments, we utilized a *gfp*-expressing strain of *Mtb* mc^{2}6206 to infect THP-1 cells, a monocyte cell line widely used in *Mtb* research.[22,23] The ability of this *Mtb* strain to express GFP allows for the visual control of macrophage phagocytosis efficacy and direct quantification of infection levels. Since this auxotrophic strain does not replicate during macrophage infection, we rationalized to use a higher than standard MOI to mimic the intracellular replication observed with wild-type *Mtb,* where the bacterial burden is known to increase by 10-fold after ~5 days of infection.[24]

Infection of nondifferentiated THP-1 monocytes at an MOI of 25 initially showed features of limited differentiation to a macrophage-like phenotype as indicated by macrophage aggregation after 3–4 days (*Fig. 1A*). THP-1 cells did not differentiate into the classic phorbol 12-myristate 13-acetate (PMA)-induced macrophage phenotype and adhered to the bottom of the wells, but rather started to increase in size and adhered to neighboring cells, thereby forming *Mtb*/macrophage aggregate structures. By day 8–10, the size of *Mtb*/macrophage aggregates built around a densely packed core of *Mtb* had increased to >100 μm (*Fig. 1B*). *Mtb*/macrophage aggregates could be directly generated in 96-well plates (*Fig. 1C–E*) or the production could be efficiently scaled up to larger flask volumes (*e.g.*, T-75 flasks) to produce sufficient material for throughput-format experiments.

The underlying idea of creating large *Mtb*/macrophage aggregate structures to study drug efficacy was to generate a biologically relevant model that resembles *in vivo* conditions, where *Mtb* is trapped and embedded within multiple layers of

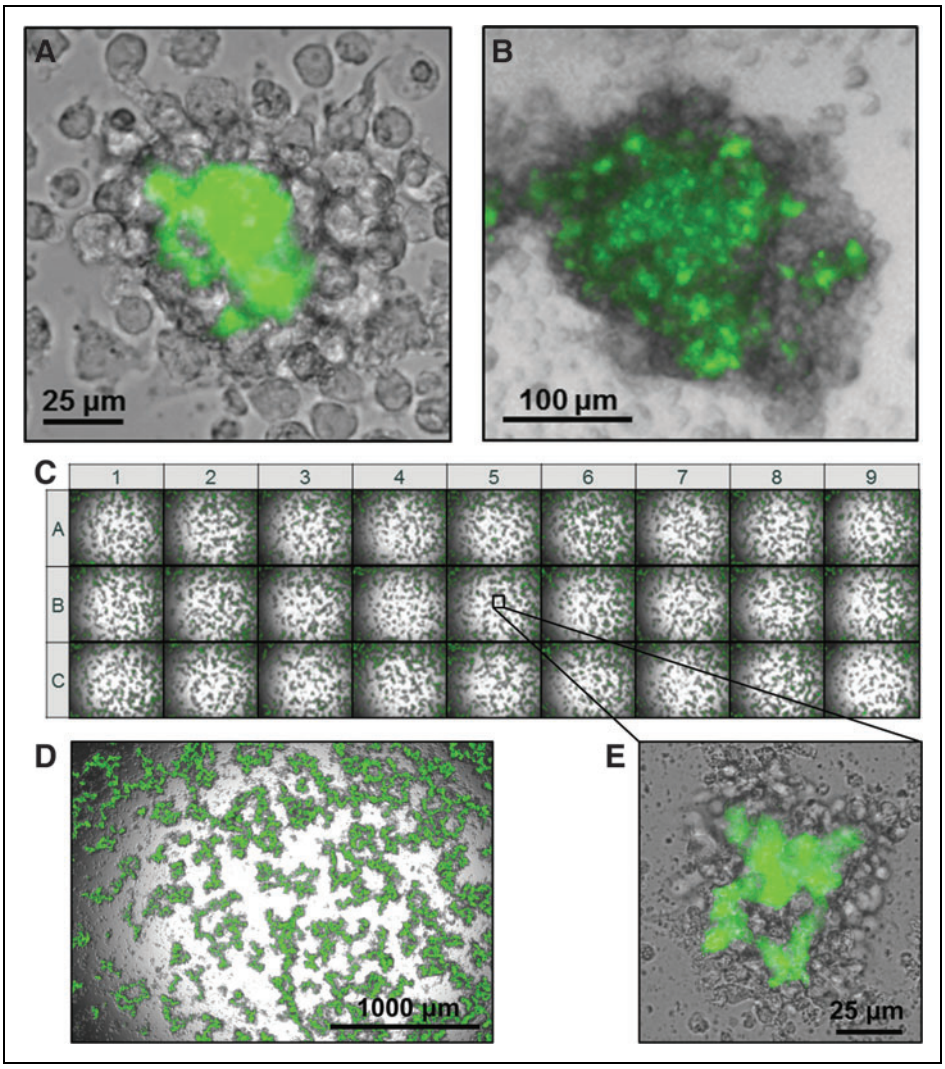

Fig. 1. An *Mtb* infection model to generate large *Mtb*/macrophage aggregate structures. THP-1 monocytes were infected with *Mtb*-GFP at an MOI of 25 and *Mtb*/macrophage aggregate formation was documented. Representative bright-field and GFP-merged images of *Mtb*-infected THP-1 aggregate structures are shown **(A)** on day 4 and **(B)** day 10 postinfection. **(C)** Generation of *Mtb*/macrophage aggregate structures in 96-well plate format. Bright-field and GFP-merged images were acquired 7 days postinfection by automated imaging. Enlarged view of images from **(D)** well A6 with 2.5×objective and **(E)** well B5 with 20×objective are shown. MOI, multiplicity of infection.

immune cells and necrotic tissue, which alter the penetration efficacy of drugs. To examine the biological relevance of this model, we probed the experimental system for the presence of a (i) central necrotic core, (ii) the containment of *Mtb* within the core of the aggregates by viable macrophages, (iii) a possibly latent *Mtb* phenotype, and (iv) the presence of viable *Mtb* residing inside macrophages. All of these parameters are important features at sites of *Mtb* infection *in vivo*.[5,25,26]

The core of the *Mtb*/macrophage aggregates contained densely packed *Mtb* (*Fig. 1B*) and dead cell material that stained positive for 7AAD (*Fig. 2A*), reproducing previously reported observations that *Mtb*-infected human macrophages form cell aggregates that show prominent features of necrosis, such as the release of DNA into the extracellular space.[27] The aggregate core was enclosed by a layer of noninfected macrophages that expressed high levels of ICAM-1 (*Fig. 2B*), an adhesion molecule known to play an essential role in *in vivo* granuloma formation,[26] where increased ICAM-1 expression during *Mtb* infection is necessary to promote cellular adhesion.[28] Functionality of the enhanced expression of surface adhesion molecules indicates tight cell–cell interactions, as confirmed by the fact that even mechanical stress (*e.g.*, rigid pipetting) did not result in relevant disintegration of the *Mtb*/macrophage aggregates. Agitation released single viable macrophages that harbored intracellular *Mtb*, which could be isolated from the aggregate structures (*Fig. 2C*). Outgrowth experiments from aggregate-derived *Mtb* revealed that almost 100% of the *Mtb* cells harvested from 11-day-old cultures were viable when compared to the inoculum on day 1 (*Fig. 2D*). Furthermore, *Mtb* extracted from the highly dense *Mtb*/macrophage aggregate core stained positive with the lipophilic dye Nile Red (*Fig. 2E*), which detects the presence of intracellular lipid bodies suggesting the possibility of latent mycobacteria.[29–31] At the least, this result indicated metabolic changes of *Mtb* following passage through these aggregate forming macrophage infection cultures.

Drug penetration into lung tissues, the primary site of *Mtb* infection and granuloma formation, is complex and involves different processes such as passive diffusion, permeation, active transport, and bulk flow.[32] Accordingly, various classes of antibiotics show different penetration properties. For instance, aminoglycosides are too polar to diffuse directly across lipid membranes, and therefore enter cells slowly by endocytosis.[33] Uptake of β-lactam antibiotics is also poor in alveolar

© MARY ANN LIEBERT, INC.

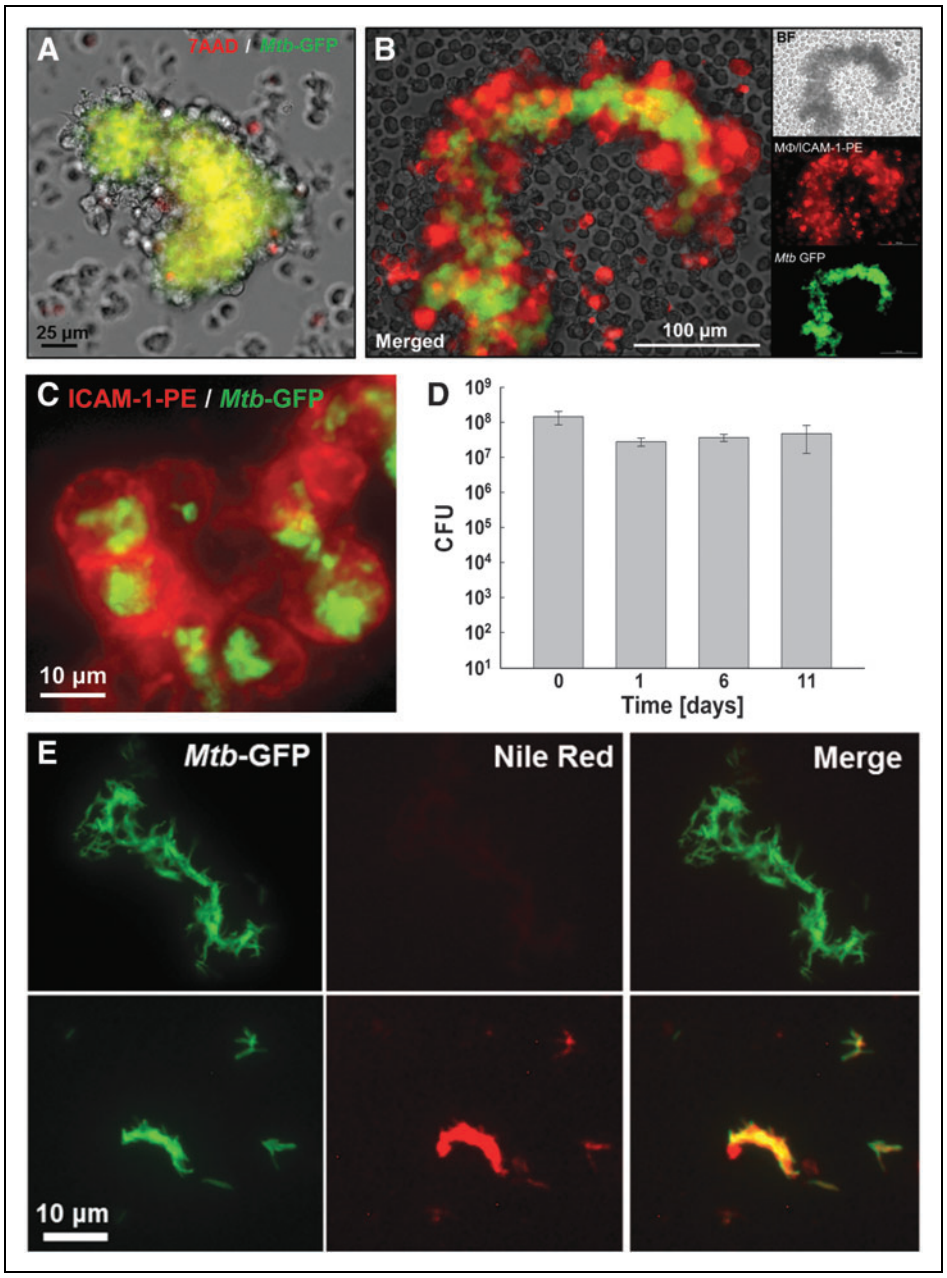

Fig. 2. Biomolecular characterization of *Mtb*/macrophage aggregate structures. **(A)** *Mtb*/macrophage aggregate structures at 2 weeks postinfection were stained with 7AAD and a representative image is shown as merged GFP (*Mtb*) and RFP (7AAD) channels with bright-field image. **(B)** *Mtb*/macrophage aggregate structures at 2 weeks postinfection were stained with α-ICAM-1-PE mAbs and representative images are shown as merged GFP and RFP channels with bright-field images, or in separate channels alone. **(C)** Representative merged *red* and *green* channel fluorescence images of a group of viable macrophages derived from *Mtb*/macrophage aggregates stained with α-ICAM-1-PE antibody (*red*) that contain intracellular *Mtb* (*green*) at 2 weeks postinfection. **(D)** Intracellular survival of *Mtb* extracted from aggregate structures over a time course of 11 days was enumerated by CFU plating. **(E)** *Mtb*-GFP from *in vitro* broth-grown single-cell cultures (*top panel*) or extracted from *Mtb*/macrophage aggregates structures (*bottom panel*) 11 days postinfection were stained with Nile Red and representative images are shown as a merge of GFP and RFP channels, or in each individual channel. 7AAD, 7-amino-actinomycin D.

macrophages.[34] Conversely, uptake of rifampicin, tetracycline, or ethambutol into alveolar macrophages is relatively faster, and quinolone levels in lung tissue are often 15–20 times higher than serum levels.[35] These pharmacological characteristics define *in vivo* drug efficacy, but are inadequately addressed by most other standard evaluation methods.

To explore whether the *Mtb*/macrophage aggregate model could improve our ability to predict the potential *in vivo* efficacy of hit or lead compounds, we tested the efficacy of several standard *Mtb* drugs against *Mtb* in *Mtb*/macrophage aggregates relative to their efficacy on *in vitro* broth-grown single-cell *Mtb* cultures. For this purpose, we used a panel of commonly used antibiotics and TB drugs for which properties such as penetration capacity into lung tissue or cerebrospinal fluid (CSF),[36–38] as well as activity against persistent *Mtb*[39] were reported (rifampicin, moxifloxacin, ciprofloxacin, streptomycin, gentamicin, cycloserine, and clarithromycin). *Mtb*/macrophage aggregates were harvested from large-scale infection cultures after 14 days, while *in vitro* broth-grown single-cell *Mtb* cultures were used as references. Thereafter, *Mtb*/macrophage aggregates or *in vitro* broth-grown single-cell *Mtb* were incubated in mycobacteria growth media (7H9 media) containing a titration of the aforementioned drugs for 5 days. As the purpose of this study is to test drug efficacy on macrophage-passaged *Mtb* aggregates that should more closely resemble *in vivo* conditions, the use of mycobacteria growth media is essential for compatibility with a growth inhibition assay to measure drug effects. Thus, we chose to use the well-characterized resazurin microtiter assay for mycobacteria growth[40] to quantify the drug susceptibility of *Mtb* derived from our *Mtb*/macrophage aggregate model in 96-well microplate

format. The eventual disintegration of macrophages in mycobacteria growth media releases *Mtb* aggregates into the medium and allows *Mtb* cells to undergo enough bacterial replication to enable sensitivity for measurement by the resazurin assay. The addition of 0.5% Tween 80 at the beginning of the resazurin incubation period would eliminate all remaining macrophages in the sample, and thus ensure that the measured metabolic activity would only be associated with *Mtb* that survived the antibiotic treatment. This was confirmed by the fact that noninfected THP-1 cells treated in the same manner did not register any metabolic activity (data not shown).

Suboptimal dosing of rifampicin is a widely recognized problem.[41–43] Rifampicin, despite being the antibiotic of choice to treat *Mtb* infection, is known to ineffectively penetrate pulmonary granulomatous lesions,[14] or only reach low concentrations in the CSF of tuberculous meningitis patients.[38] Consistent with these reports, the MIC of rifampicin was >10-fold higher in *Mtb* from *Mtb*/macrophage aggregate cultures compared to *in vitro* broth-grown *Mtb* control cultures, as determined by susceptibility killing curves (*Fig. 3A* and *Table 3*). A possible explanation for this finding could be that the large size (>800 Da) and lipophilic properties[37] may result in incomplete rifampicin penetration through the many layers of cell membranes and debris that create the *Mtb*/macrophage aggregate structures, and particularly into the necrotic core of the aggregates.

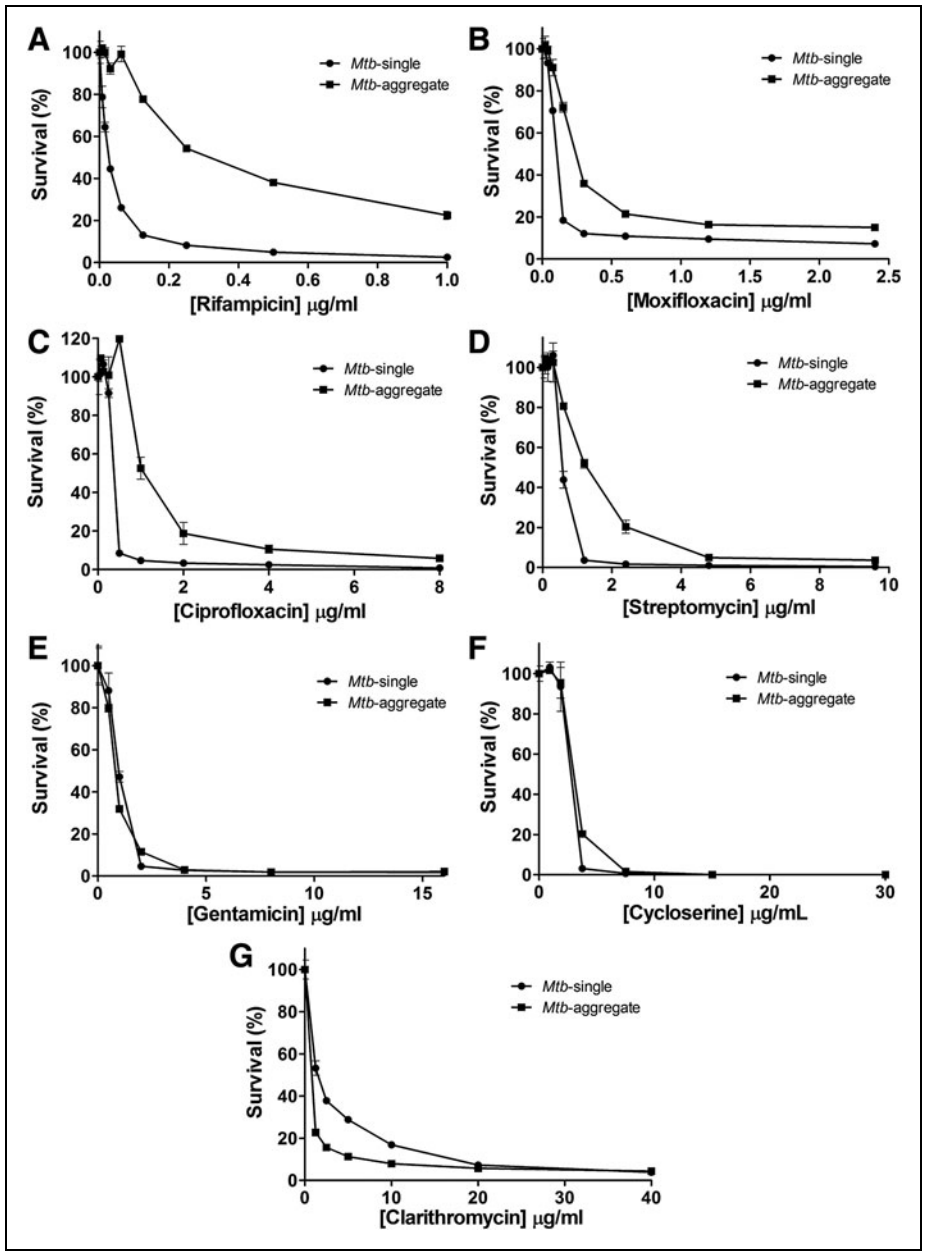

Fig. 3. *Mtb* drug sensitivity profiles for rifampicin and other antibiotics in the *Mtb*/macrophage aggregate model. Drug susceptibility of *Mtb* derived from *Mtb*/macrophage aggregate cultures (*Mtb*-aggregate) to **(A)** rifampicin, **(B)** moxifloxacin, **(C)** ciprofloxacin, **(D)** streptomycin, **(E)** gentamicin, **(F)** cycloserine, and **(G)** clarithromycin compared to *in vitro* broth-grown single-cell *Mtb* cultures (*Mtb*-single). All data are represented as killing curves indicating the % survival as normalized to maximal bacterial growth in the absence of drugs and expressed as the mean ± standard deviation of three independent experiments.

To test the idea that the *Mtb*/macrophage aggregates could affect drug penetration, we next tested the ability of the fluoroquinolone moxifloxacin to exert its anti-*Mtb* activity in this model. Moxifloxacin was reported to penetrate granulomatous lesions more effectively than rifampicin.[14,15] Similar to rifampicin, moxifloxacin provides satisfactory activity against persistent *Mtb* in *in vitro* models.[39] Differences in the relative ability of these two antibiotics to act against *Mtb* derived from macrophage aggregates or *in vitro* broth-grown cultures should thus be mostly attributable to tissue diffusion characteristics. *Mtb* in the *Mtb*/macrophage aggregate cultures indeed exhibited a 4- to 8-fold relative increase in tolerance to moxifloxacin (*Fig. 3B* and *Table 3*). Similar findings were made for ciprofloxacin, another

© MARY ANN LIEBERT, INC.

Table 3. MIC90 of Drugs Against *Mtb* from *Mtb*/Macrophage Aggregates and Nonreplicating Latent *Mtb* Compared to Active Broth-Grown *Mtb*

	MIC (μg/mL)			
Drugs	*Mtb*-single	*Mtb*-aggregate	*Mtb*-latent	Literature[a]
Rifampicin	0.125	>1.0	0.5	0.16
Moxifloxacin	0.3	1.2–2.4	0.3–0.6	0.25
Ciprofloxacin	0.5	4	0.5	0.5
Streptomycin	1.2	4.8	2.4	0.35
Gentamicin	2.0	2.0	ND	6.0
Cycloserine	3.75	7.5	ND	15.6
Clarithromycin	20	10	ND	26

[a]MIC values against *in vitro*-grown *Mtb* reported in the literature.[40,50]
ND, not determined.

fluoroquinolone (*Fig. 3C* and *Table 3*). Increased tissue penetration compared to rifampicin could possibly be the result of different pharmacological properties, with fluoroquinolone compounds exhibiting moderate lipophilicity and being of lower molecular weight (~300 Da).[37]

Streptomycin, a first-line TB drug belonging to the class of aminoglycoside antibiotics that are known to poorly diffuse across membranes,[33] is relative large (>500 Da) and hydrophilic,[37] properties that hinder penetration into the CSF.[36,38] These properties correlated well with the fourfold increase in MIC to streptomycin for *Mtb* from aggregate cultures, relative to *in vitro* broth-grown single-cell cultures (*Fig. 3D* and *Table 3*). Although aminoglycosides generally exhibit poor tissue penetration, gentamicin concentrations in the alveolar lining fluid of patients were found to correlate well with serum concentrations with a penetration ratio of 0.32.[44] Consistent with this physiological finding and not with its chemical properties, *Mtb* in *Mtb*/macrophage aggregate cultures showed no difference in susceptibility to gentamicin, relative to *in vitro* broth-grown *Mtb* (*Fig. 3E* and *Table 3*).

Last, consistent with its reported excellent CSF penetration properties[36] and small size (~100 Da), cycloserine sensitivity was unchanged against *Mtb* in *Mtb*/macrophage aggregate cultures when compared to *in vitro* broth-grown *Mtb* (*Fig. 3F* and *Table 3*). Also, susceptibility of *Mtb* from aggregate cultures to clarithromycin, a macrolide antibiotic, was similar or even slightly increased relative to *in vitro* broth-grown *Mtb* cultures (*Fig. 3G* and *Table 3*), a result that is consistent with its pharmacokinetic properties that show high tissue concentrations relative to serum concentrations, indicating effective diffusion into lung tissue and phagocytes.[32,45] In summary, these results suggest that the data obtained using the *Mtb*/macrophage aggregate model are likely good predictors of drug efficacy in a physiologically relevant setting where tissue penetration is critical.

As revealed by Nile Red stains and CFU enumeration experiments (*Fig. 2D, E*), the introduced *Mtb*/macrophage aggregate model produces nonreplicating *Mtb* that has accumulated large amounts of lipid bodies, features suggestive of a latent infection phenotype.[31] To investigate whether it is possible to determine the relative contributions of (i) a latent *Mtb* infection status[29,46] or (ii) the diffusion barrier of the core structure, to the increased drug tolerance of *Mtb* observed in the *Mtb*/macrophage aggregate model, we determined drug susceptibility killing curves against nonreplicating latent *Mtb* cells generated by the commonly used nutrient starvation method.[9,47] In these latent *Mtb* cultures, tolerance to the four drugs (rifampicin, moxifloxacin, ciprofloxacin, streptomycin) that showed increased MICs against *Mtb* from *Mtb*/macrophage aggregates were relatively unchanged with the exception of rifampicin, which showed a modest two to fourfold increase compared to broth-grown *Mtb* cultures (*Fig. 4A–D* and *Table 3*). This result is consistent with reports of increased rifampicin resistance in long-term persistent *Mtb* that show features of latency or nonreplicating phenotype.[9,29,46] Furthermore, this suggests that the >10-fold increase in the MIC of rifampicin against *Mtb* from *Mtb*/macrophage aggregates is mainly modulated by the altered drug diffusion properties of the *Mtb*/macrophage aggregates, and only to a lesser extent by a latent infection status.

As with most throughput assays, the *Mtb*/macrophage aggregate model is a simplification and reductionist approach to an otherwise complex biological system, and thus would not suffice as a complete granuloma model. However, the following key features of the *Mtb*/macrophage aggregate structures: (i) a highly dense necrotic core containing *Mtb* with a high content of intracellular lipid bodies[29–31] (*Fig. 2E*), (ii) the presence of viable macrophages that harbor intracellular, viable *Mtb* (*Fig. 2C, D*), and (iii) the tight, multilayer envelope of noninfected macrophages surrounding the infected core of the aggregate structure (*Fig. 1*) were sufficient to produce *in vitro* drug efficacy data with very good correlation to reported *in vivo* tissue penetration data.[14,15,38,42] Drugs like cycloserine, clarithromycin or gentamicin, known to effectively penetrate into tissues, exhibited no efficacy differences in the *Mtb*/macrophage aggregate model when compared to *in vitro* broth-grown *Mtb* cultures, while the reduced tissue penetration capacity of rifampicin or moxifloxacin was efficiently predicted by the *Mtb*/macrophage aggregate model (*Fig. 3A, B*).

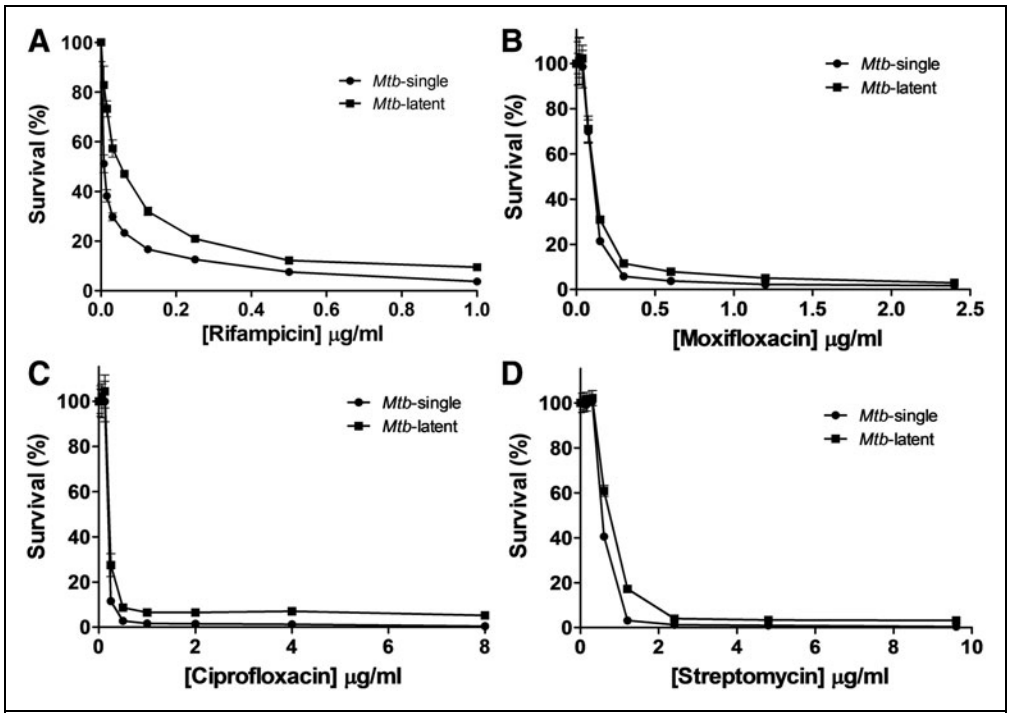

Fig. 4. Drug susceptibility of latent *Mtb* compared to actively replicating broth-grown cultures. Drug susceptibility of *Mtb* from nutrient starvation derived nonreplicating *Mtb* (*Mtb*-latent) to **(A)** rifampicin, **(B)** moxifloxacin, **(C)** ciprofloxacin, and **(D)** streptomycin compared to active growing broth-grown single-cell *Mtb* cultures (*Mtb*-single). All data are represented as killing curves indicating the % survival as normalized to maximal bacterial growth in the absence of drugs and expressed as the mean ± standard deviation of three independent experiments.

Drug susceptibility of intracellular *Mtb* differs from *in vitro* broth-grown *Mtb* as it has been shown that increased drug concentrations are necessary to be effective against intracellular mycobacteria.[43,48] Our data are in strong agreement with these findings showing that rifampicin, streptomycin, and fluoroquinolones require higher concentrations to inhibit growth of intracellular *Mtb*.[48] Our model further demonstrates that rifampicin has the largest discrepancy in efficacy against *Mtb* from *Mtb*/macrophage aggregates compared to *in vitro* broth-grown *Mtb*, while streptomycin and fluoroquinolones show smaller differences, all of which are consistent with previously established drug efficacy testing against intracellular *Mtb*.[48] This would suggest that our model is indeed reflective of or even comparable to other intracellular *Mtb* drug susceptibility infection models. In addition to these valuable and informative high-content screening methods against intracellular *Mtb*,[10–12,48] recent development of an *in vitro* granuloma-based *Mtb* drug susceptibility phenotyping confirms that drug concentration requirements are altered within granulomas,[49] which further supports findings from our simplified *Mtb*/macrophage aggregate model. Therefore, that our model is able to produce drug efficacy data consistent with several intracellular *Mtb* infection models shows its promise as an alternative method to quickly and reliably assess drug efficacy against *Mtb* during the early drug development process. Importantly, our infection model is advantageous in (i) its ability to generate unlimited amounts of *Mtb*/macrophages aggregates (*in vitro* granulomas) necessary for high-throughput screening compared to using primary macrophages from donors, (ii) is BSL-2 compatible, thus saving valuable time and money, and (iii) does not require high-end instrumentation compatible with high-content imaging analysis.

As such, our alternative model would address one of the key problems in *Mtb* drug development, which is the inefficient correlation of *in vitro* drug efficacy of currently used screening methods[7] with *in vivo* outcomes. Our data suggest that this disconnect would be, in particular, a problem for the ability of some screening models to predict drug penetration efficacy of the candidate compounds into the granulomatous or necrotic tissues at the site of *Mtb* infection. The generation of truly authoritative and accurate drug penetration profiles in *in vivo* lung lesions and granulomas[13–15] will remain limited to a few laboratories in the world, and due to specific instrumentation requirements, these methods are not amenable to throughput analysis early in the drug development process. Our model would provide a cost-effective, rapid, and BSL2-compatible alternative with good predictive capability for the *in vivo* ability of antibiotics to penetrate into key tissues such as the lung or the CSF.[32,36–38,45]

ACKNOWLEDGMENTS

We thank Dr. William Jacobs (Albert Einstein University, New York) for kindly providing *M. tuberculosis* mc^{2}6206. This work was funded, in part, by NIH grants R01-AI104499 and R21-AI116188 to O.K. and R01-AI104952 to F.W. Parts of the work were performed in the UAB CFAR BSL-3 facilities and by the UAB CFAR Flow Cytometry Core/Joint UAB Flow Cytometry Core, which are funded by NIH/NIAID P30 AI027767 and by NIH 5P30 AR048311.

© MARY ANN LIEBERT, INC.

AUTHOR CONTRIBUTIONS

A.S., F.W., M.N., O.K., and J.S. conceived and designed experiments and analyzed data; K.S., V.H., A.S., and J.S. performed experiments; and F.W., M.N., O.K., and J.S. wrote and edited the article.

DISCLOSURE STATEMENT

No competing financial interests exist.

REFERENCES

1. Bass JB, Jr, Farer LS, Hopewell PC, *et al.*: Treatment of tuberculosis and tuberculosis infection in adults and children. American Thoracic Society and The Centers for Disease Control and Prevention. *Am J Respir Crit Care Med* 1994; 149:1359–1374.
2. Dartois V: The path of anti-tuberculosis drugs: From blood to lesions to mycobacterial cells. *Nat Rev Microbiol* 2014;12:159–167.
3. Ramakrishnan L: Revisiting the role of the granuloma in tuberculosis. *Nat Rev Immunol* 2012;12:352–366.
4. Brennan PJ, Nikaido H: The envelope of mycobacteria. *Annu Rev Biochem* 1995;64:29–63.
5. Gupta A, Kaul A, Tsolaki AG, Kishore U, Bhakta S: Mycobacterium tuberculosis: Immune evasion, latency and reactivation. *Immunobiology* 2012;217:363–374.
6. Ekins S, Pottorf R, Reynolds RC, Williams AJ, Clark AM, Freundlich JS: Looking back to the future: Predicting in vivo efficacy of small molecules versus Mycobacterium tuberculosis. *J Chem Inf Model* 2014;54:1070–1082.
7. Evangelopoulos D, da Fonseca JD, Waddell SJ: Understanding anti-tuberculosis drug efficacy: Rethinking bacterial populations and how we model them. *Int J Infect Dis* 2015;32:76–80.
8. Lechartier B, Rybniker J, Zumla A, Cole ST: Tuberculosis drug discovery in the post-post-genomic era. *EMBO Mol Med* 2014;6:158–168.
9. Sarathy J, Dartois V, Dick T, Gengenbacher M: Reduced drug uptake in phenotypically resistant nutrient-starved nonreplicating *Mycobacterium tuberculosis*. *Antimicrob Agents Chemother* 2013;57:1648–1653.
10. Sorrentino F, Gonzalez Del Rio R, Zheng X, *et al.*: Development of an intracellular screen for new compounds able to inhibit *Mycobacterium tuberculosis* growth in human macrophages. *Antimicrob Agents Chemother* 2015;60:640–645.
11. Queval CJ, Song OR, Delorme V, *et al.*: A microscopic phenotypic assay for the quantification of intracellular mycobacteria adapted for high-throughput/high-content screening. *J Vis Exp* 2014:e51114.
12. Stanley SA, Barczak AK, Silvis MR, *et al.*: Identification of host-targeted small molecules that restrict intracellular Mycobacterium tuberculosis growth. *PLoS Pathog* 2014;10:e1003946.
13. Prideaux B, Via LE, Zimmerman MD, *et al.*: The association between sterilizing activity and drug distribution into tuberculosis lesions. *Nat Med* 2015;21:1223–1227.
14. Kjellsson MC, Via LE, Goh A, *et al.*: Pharmacokinetic evaluation of the penetration of antituberculosis agents in rabbit pulmonary lesions. *Antimicrob Agents Chemother* 2012;56:446–457.
15. Prideaux B, Dartois V, Staab D, *et al.*: High-sensitivity MALDI-MRM-MS imaging of moxifloxacin distribution in tuberculosis-infected rabbit lungs and granulomatous lesions. *Anal Chem* 2011;83:2112–2118.
16. Sampson SL, Dascher CC, Sambandamurthy VK, *et al.*: Protection elicited by a double leucine and pantothenate auxotroph of *Mycobacterium tuberculosis* in guinea pigs. *Infect Immun* 2004;72:3031–3037.
17. Steinhauer K, Eschenbacher I, Radischat N, Detsch C, Niederweis M, Goroncy-Bermes P: Rapid evaluation of the mycobactericidal efficacy of disinfectants in the quantitative carrier test EN 14563 by using fluorescent *Mycobacterium terrae*. *Appl Environ Microbiol* 2010;76:546–554.
18. Davis JM, Ramakrishnan L: The role of the granuloma in expansion and dissemination of early tuberculous infection. *Cell* 2009;136:37–49.
19. Speer A, Shrestha TB, Bossmann SH, *et al.*: Copper-boosting compounds: A novel concept for antimycobacterial drug discovery. *Antimicrob Agents Chemother* 2013;57:1089–1091.
20. Vilcheze C, Hartman T, Weinrick B, Jacobs WR, Jr.: *Mycobacterium tuberculosis* is extraordinarily sensitive to killing by a vitamin C-induced Fenton reaction. *Nat Commun* 2013;4:1881.
21. Dalecki AG, Haeili M, Shah S, *et al.*: Disulfiram and copper ions kill *Mycobacterium tuberculosis* in a synergistic manner. *Antimicrob Agents Chemother* 2015;59:4835–4844.
22. Stokes RW, Doxsee D: The receptor-mediated uptake, survival, replication, and drug sensitivity of *Mycobacterium tuberculosis* within the macrophage-like cell line THP-1: A comparison with human monocyte-derived macrophages. *Cell Immunol* 1999;197:1–9.
23. Jordao L, Bleck CK, Mayorga L, Griffiths G, Anes E: On the killing of mycobacteria by macrophages. *Cell Microbiol* 2008;10:529–548.
24. Danilchanka O, Sun J, Pavlenok M, *et al.*: An outer membrane channel protein of *Mycobacterium tuberculosis* with exotoxin activity. *Proc Natl Acad Sci USA* 2014;111:6750–6755.
25. Swaim LE, Connolly LE, Volkman HE, Humbert O, Born DE, Ramakrishnan L: *Mycobacterium marinum* infection of adult zebrafish causes caseating granulomatous tuberculosis and is moderated by adaptive immunity. *Infect Immun* 2006;74:6108–6117.
26. Saunders BM, Frank AA, Orme IM: Granuloma formation is required to contain bacillus growth and delay mortality in mice chronically infected with *Mycobacterium tuberculosis*. *Immunology* 1999;98:324–328.
27. Wong KW, Jacobs WR, Jr.: *Mycobacterium tuberculosis* exploits human interferon gamma to stimulate macrophage extracellular trap formation and necrosis. *J Infect Dis* 2013;208:109–119.
28. DesJardin LE, Kaufman TM, Potts B, Kutzbach B, Yi H, Schlesinger LS: *Mycobacterium tuberculosis*-infected human macrophages exhibit enhanced cellular adhesion with increased expression of LFA-1 and ICAM-1 and reduced expression and/or function of complement receptors, FcgammaRII and the mannose receptor. *Microbiology* 2002;148:3161–3171.
29. Kapoor N, Pawar S, Sirakova TD, Deb C, Warren WL, Kolattukudy PE: Human granuloma *in vitro* model, for TB dormancy and resuscitation. *PLoS One* 2013;8:e53657.
30. Garton NJ, Christensen H, Minnikin DE, Adegbola RA, Barer MR: Intracellular lipophilic inclusions of mycobacteria in vitro and in sputum. *Microbiology* 2002;148:2951–2958.
31. Daniel J, Maamar H, Deb C, Sirakova TD, Kolattukudy PE: *Mycobacterium tuberculosis* uses host triacylglycerol to accumulate lipid droplets and acquires a dormancy-like phenotype in lipid-loaded macrophages. *PLoS Pathog* 2011; 7:e1002093.
32. Honeybourne D: Antibiotic penetration into lung tissues. *Thorax* 1994;49:104–106.
33. Tulkens PM: Intracellular pharmacokinetics and localization of antibiotics as predictors of their efficacy against intraphagocytic infections. *Scand J Infect Dis Suppl* 1990;74:209–217.
34. Stewart SM, Fisher M, Young JE, Lutz W: Ampicillin levels in sputum, serum, and saliva. *Thorax* 1970;25:304–311.
35. Hand WL, Corwin RW, Steinberg TH, Grossman GD: Uptake of antibiotics by human alveolar macrophages. *Am Rev Respir Dis* 1984;129:933–937.
36. Donald PR: Cerebrospinal fluid concentrations of antituberculosis agents in adults and children. *Tuberculosis (Edinb)* 2010;90:279–292.
37. Nau R, Sorgel F, Eiffert H: Penetration of drugs through the blood-cerebrospinal fluid/blood-brain barrier for treatment of central nervous system infections. *Clin Microbiol Rev* 2010;23:858–883.
38. Ellard GA, Humphries MJ, Allen BW: Cerebrospinal fluid drug concentrations and the treatment of tuberculous meningitis. *Am Rev Respir Dis* 1993;148:650–655.
39. Zhang Y, Yew WW, Barer MR: Targeting persisters for tuberculosis control. *Antimicrob Agents Chemother* 2012;56:2223–2230.
40. Collins L, Franzblau SG: Microplate alamar blue assay versus BACTEC 460 system for high-throughput screening of compounds against *Mycobacterium tuberculosis* and *Mycobacterium avium*. *Antimicrob Agents Chemother* 1997; 41:1004–1009.

41. Diacon AH, Patientia RF, Venter A, *et al.*: Early bactericidal activity of high-dose rifampin in patients with pulmonary tuberculosis evidenced by positive sputum smears. *Antimicrob Agents Chemother* 2007;51:2994–2996.
42. van Ingen J, Aarnoutse RE, Donald PR, *et al.*: Why do we use 600 mg of rifampicin in tuberculosis treatment? *Clin Infect Dis* 2011;52:e194–e199.
43. Hartkoorn RC, Chandler B, Owen A, *et al.*: Differential drug susceptibility of intracellular and extracellular tuberculosis, and the impact of P-glycoprotein. *Tuberculosis (Edinb)* 2007;87:248–255.
44. Panidis D, Markantonis SL, Boutzouka E, Karatzas S, Baltopoulos G: Penetration of gentamicin into the alveolar lining fluid of critically ill patients with ventilator-associated pneumonia. *Chest* 2005;128:545–552.
45. Fish DN, Gotfried MH, Danziger LH, Rodvold KA: Penetration of clarithromycin into lung tissues from patients undergoing lung resection. *Antimicrob Agents Chemother* 1994;38:876–878.
46. Deb C, Lee CM, Dubey VS, *et al.*: A novel in vitro multiple-stress dormancy model for Mycobacterium tuberculosis generates a lipid-loaded, drug-tolerant, dormant pathogen. *PLoS One* 2009;4:e6077.
47. Gengenbacher M, Rao SP, Pethe K, Dick T: Nutrient-starved, non-replicating Mycobacterium tuberculosis requires respiration, ATP synthase and isocitrate lyase for maintenance of ATP homeostasis and viability. *Microbiology* 2010; 156:81–87.
48. Christophe T, Jackson M, Jeon HK, *et al.*: High content screening identifies decaprenyl-phosphoribose 2′ epimerase as a target for intracellular antimycobacterial inhibitors. *PLoS Pathog* 2009;5:e1000645.
49. Silva-Miranda M, Ekaza E, Breiman A, *et al.*: High-content screening technology combined with a human granuloma model as a new approach to evaluate the activities of drugs against *Mycobacterium tuberculosis*. *Antimicrob Agents Chemother* 2015;59:693–697.
50. Gillespie SH, Billington O: Activity of moxifloxacin against mycobacteria. *J Antimicrob Chemother* 1999;44:393–395.

Address correspondence to:
Jim Sun, PhD
Department of Microbiology
University of Alabama at Birmingham
845 19th Street South, BBRB 530
Birmingham, AL 35294-2172

E-mail: jsun14@uab.edu

Olaf Kutsch, PhD
Department of Medicine
University of Alabama at Birmingham
845 19th Street South, BBRB 510
Birmingham, AL 35294-2172

E-mail: okutsch@uab.edu

Abbreviations Used

7AAD = 7-amino-actinomycin D
CSF = cerebrospinal fluid
FBS = fetal bovine serum
MIC = minimal inhibitory concentration
MOI = multiplicity of infection
Mtb = *Mycobacterium tuberculosis*
TB = tuberculosis

© MARY ANN LIEBERT, INC.